International
Progress Report

IPR-01-42

Äspö Hard Rock Laboratory

TRUE Block Scale project
Preliminary characterisation stage

September 1998 Structural model; Update using caracterisation data from KI0023B

Jan Hermanson

Golder Grundteknik

September 1998

Svensk Kärnbränslehantering AB
Swedish Nuclear Fuel
and Waste Management Co
Box 5864
SE-102 40 Stockholm Sweden
Tel +46 8 459 84 00
Fax +46 8 661 57 19

Äspö Hard Rock
Laboratory

Report no.	No.
IPR-01-42	F56K
Author	Date
Hermanson	
Checked by	Date
Approved	Date
Christer Svemar	02-08-23

Äspö Hard Rock Laboratory

TRUE Block Scale project
Preliminary characterisation stage

September 1998 Structural model; Update using caracterisation data from KI0023B

Jan Hermanson

Golder Grundteknik

September 1998

Keywords: True, geology, structural model

Abstract

This report presents an update of the Oct'97 structural model of the TRUE Block Scale volume. This update includes new geological, geophysical and hydraulic information from borehole KI0023B as well as extensive re-workings of data from boreholes KA2563A, KA2511A, KA3510A and KI0025F.

The structural geology of the major structures in the block are subdivided in a simple geological classification system. The subdivision is based on four types of geological structures; fractures, faults, swarms and zones, in an attempt to make the heterogeneity of the geology in many of the structures comprehensible. This terminology has then been used in conjunction with hydraulic data to support the variable hydraulic characteristics in the block.

The major findings from this update is that none of the existing structures in the Oct'97 model could be rejected on the grounds of the new information obtained from KI0023B. Zone NE-2 (Rhén et al 1997) have not been confirmed and has to be interpreted with care. The heterogeneity of the hydraulic characteristics of structure 19 have been confirmed by the varying geological signature in the observed borehole intercepts. This is similar in many of the identified structures in the block.

One new structure, #13, has been defined. This structure is a parallel fault to structure 20 and exhibits similar geological and hydraulic characteristics as structure 20. With the aid of preliminary results from the interference test program by Andersson et al (1998) a local set of structures have been found that are partly hydraulically isolated from the rest of the block. This local system consists of structures 9, 13 and 20 and are localised in the centre part of the block.

Sammanfattning

Den här rapporten presenterar en uppdatering av Oktober modellen av Hermanson (1997). Uppdateringen omfattar geologiska, geofysiska och hydrauliska data från borrningen av KI0023B. Vidare så har befintliga data från borrhål KA2563A, KA2511A, KA3510A och KI0025F bearbetats och återanvänts i uppdateringen.

Denna studie presenterar de identifierade strukturerna med en ny typ av strukturgeologisk klassificering. Den består av en identifiering av fyra förenklade typer av strukturer i form av sprickor, förkastningar, spricksvärmar och zoner. Klassificeringen är gjord för att beskriva heterogeniteten i geologin i de identifierade strukturerna. Den geologiska terminologin har sedan använts som hjälp vid förklaring av den hydrauliska bilden från interferenstesterna av Andersson m.fl. (1998).

Ingen av de existerande strukturerna identifierade av Hermanson (1997) har kunnat förkastas utifrån den nya informationen i borrhål KI0023B. Zon NE-2 (Rhén m.fl. 1997) har dock ej kunnat bekräftats varför den är att betrakta som osäker. Den geologiska heterogeniteten som kan observeras i de identifierade intercepten i struktur 19 förklarar väl den heterogena hydrauliska bilden som uppträder vid interferensförsöken. Detta är liknande i flera av de identifierade strukturerna i blocket.

En ny struktur, nr 13, har identifierats. Denna struktur är parallell med struktur 20 och har liknande geologiska och hydrauliska egenskaper. Med hjälp av preliminära resultat från interferensförsöken (Andersson m.fl. 1998) är det möjligt att identifiera tre strukturer som formar ett lokalt, delvis hydrauliskt avskärmat nätverk i centrum av blocket. Detta lokala nätverk består av strukturerna 9, 13 och 20.

Contents

List of figures

List of tables

1. Introduction

During 1996 and early 1997, a series of three boreholes, KA2563A, KA3510A and KI0025F have been drilled from the I-tunnel at L=3/510 m in the access tunnel and from the access ramp at 2/500 m. These boreholes together with an existing borehole, KA2511A, have been characterised using different geological, geophysical and hydrogeological methods (Winberg 1997). Based on collected data from the boreholes and from the mapping of the nearby tunnel segment, the structural model of the block has been updated in sequence. The most recent deterministic structural model (Oct '97-model) is reported by Hermanson (1998). In late 1997 another borehole was drilled from the I-tunnel, KI0023B, which has then been characterised by similar geological and hydrological methods.

This report presents an update of the Oct '97 model using data from the borehole investigation and activities during the drilling of KI0023B. This updated structural model replaces all earlier structural models and is presented with comprehensive tables and conceptual visualisations of the interpreted structures in the TRUE block. The main aim for the structural model update is to simplify the complexity of the geology in the block into a comprehensible numbers of structures to establish a base around which experimental design and numerical model work can be performed. Preliminary results of the performed interference tests have been used in interpretations of the connectivity of the system.

The following new sources of investigation data has been utilised

- Compilation of activities and events during drilling of KI0023B by Nilsson (1998)
- BIPS interpretation of KI0023B by Stråhle on CD-ROM (1998)
- Results from borehole radar measurements in KI0023B by Carlsten (1998)
- Detailed flow logging in core borehole KI0023B using a double packer system by Gentzschein (1998)
- Preliminary results from interference tests as reported by Winberg 980626 and by Andersson et al (1998).
- Preliminary results from the Vertical Seismic Profile investigation in the TRUE block performed by Cosma et al (1998)

A major part of the previous sources of investigation data have been revisited in the process of updating the structural model as new data has shed light over previous interpretations:

Geophysical investigations:

Radar invetigations in boreholes KA2563A, KA2511A, KA3510A and KI0025F by Carlsten (1996-1998) and Olsson (1994).

Crosshole seismic investigation in boreholes KA2563A and KA2511A by Heikkinen et al (1997).

Geological investigations:

Drilling event logs for boreholes KA2563A, KA3510A and KI0025F by Nilsson and Winberg (1996-1998)

BIPS analysis on CD-ROM in boreholes KA2563A, KA2511A, KA3510A and KI0025F by Stråhle (1996-1998).

Hydrological investigations:

Detailed flow logging in boreholes KA2563A, KA3510A and KI0025F using a double packer system by Gentzschein (1996-1997).

Response patterns during drilling of KA2563A, KA3510A and KI0025F presented in various TRUE Block Scale PM's by Winberg (1996-1998).

Based not only on the new information from KI0023B, but also from the condense database of possible water-bearing structures the following hypotheses are tested:

Can any of the defined structures in Hermanson (1998) be explained by other than planar features or by new or different intercepts?

Do sub-horizontal structures act as major hydraulic pathways?

An updated structural geological interpretation of the TRUE Block Scale structures is given in Chapter 2 and 3 with comprehensive tables and a conceptual model of major structures. The general geology of the volume is only briefly covered in this report. A more elaborate description of the general geology can be found in Hermanson (1997).Structural geology of the studied block

The lithology of the studied block consists of Äspö Diorite intersected by a number of fine-grained granites and a few greenstone bodies. The abundance of fine-grained granite in relation to the host rock (diorite) is 12% and greenstone 1% which is similar to the general picture in the HRL. The central area of the block is intersected by a group of sub-horizontal aplites of variable thickness and of variable extent. There are indications that greenstones occur in conjunction with some of the aplitic bodies.

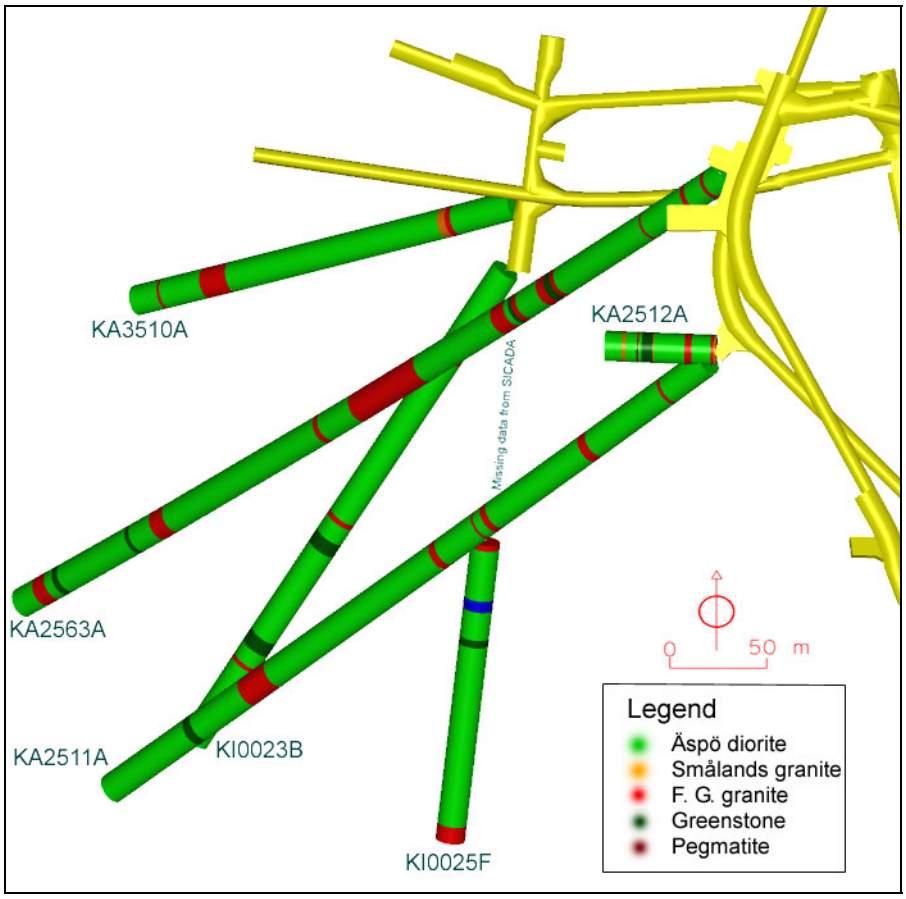

Figure 1-1 *Lithology along the TRUE Block Scale boreholes.*

Fracture orientations in all boreholes can be subdivided into three fairly well defined sets, steeply dipping NW and NNE trending and a sub-horizontal set. The sub-horizontal fracturing is most pronounced in KA2511A, whereas few sub-horizontal fractures are intersected in KI0025F and KI0023B as seen in Figure 1-2.

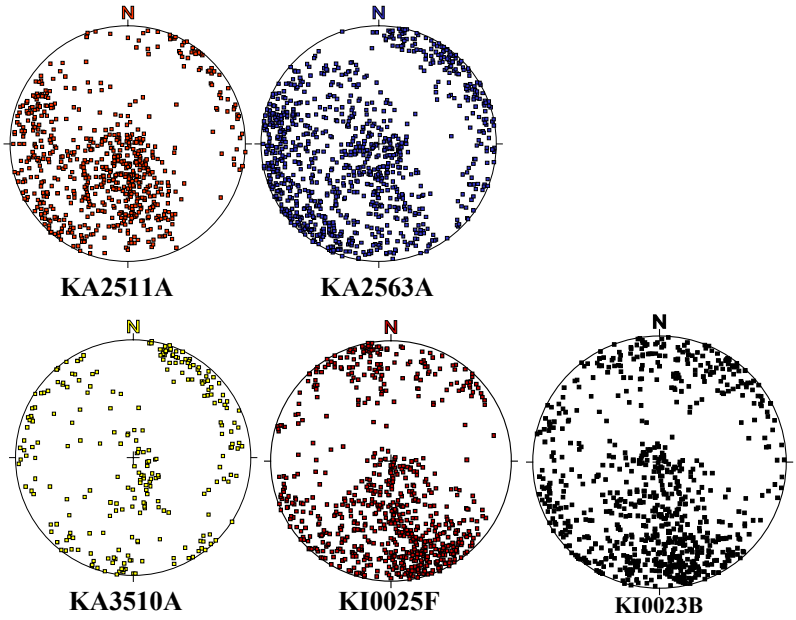

Figure 1-2 *Fracture orientations in the TRUE Block Scale boreholes.*

Note that the apparent orientation in Figure 1-2 is influenced by a bias in orientation, which originates from sampling the 3 D network with a linear object such as a borehole.

Larger sections of greenstone occur in two parts of KA2563A at around 100 m and around 300 m, and at depth in KA2511A. Smaller patches are seen i all boreholes. Greenstone has been interpreted to be gently dipping large scale thin sheets from surface observations (Talbot et al. 1990). If aplites are associated with greenstones at the surface, they may also influence the orientation of the aplites at depth. Based on this assumption it is argued that the bodies of fine-grained granite locally follow a gently dipping sheet, or several heterogeneous sheets of greenstone. The contact zone between greenstone and the host rock are often faulted with calcite fillings, at times idiomorphic in character. Contacts between aplites and host rock can be fractured, as is observed in at least one case (Structure 16) a > 0.5 m wide gently dipping fracture zone. Most other larger structures, faults and zones are interpreted as being steep, based on the orientation of seismic and radar reflections as well as fractures in the centre or on the border of the structures.

No new information from the southern and northern boundary zones, NE-1, EW-3 and EW-1 respectively have been collected within the framework of the performed characterisation.

2. Summary of structural indications in the True Block Scale volume

Structures found in the TRUE Block Scale volume can be described based on many different geological and hydraulic indications. In this report we have, in the process of finding and defining hydraulically active geological structures, used all available information from geophysical, geological and hydraulic investigations.

A compilation of the major structural information from the available drillings has been performed in an attempt to condense the accumulated comprehensive database of geological information. The compilation has been performed on the drillcore and on the BIPS aiming to extract as many of the hydraulically active structures as possible. It is of course impossible to know which structure that actually conduct water. Voids and open fractures can be distinguished from the BIPS log and correlated with the drill core and are interpreted as being potentially conductive. It is not possible on geological grounds only to extinguish which of these fractures that really contributes to the measured conductive network. This data set is thus complemented with information from geophysical and hydrological investigations to provide information to extract structures for the conceptual model. The compilation of background data on open fractures is listed in Appendix 1.

The extracted structures are presented in a conceptual model, visualised simply as hatched lines coloured after their geological signature. A table illustrating the individual intercepts of each structure is presented in Table 2-2. The structures included in the conceptual model represent the most prominent fractures, faults, swarms and zones intersecting the target volume. Comprehensive information explaining all indications and describing the interpretations are given below and in tables 3-3 to 3-7.

We have chosen to identify four types of structures based on a geological signature. At this stage in the project when the degree of detail is yet limited, it has been considered justified to simplify the identification of geological structures to four types, i.e. fractures, faults, swarms and zones. The classification is explained in Table 2-1 and in Figure 2-1. The structural geological model is presented in Figure 2-2 as differently coloured hatched lines, where red represent fractures, blue faults, green swarms and dark yellow zones. It is important to note that most of the identified structures shown in the conceptual model, in Figure 2-2, are interpreted to be groups or close networks of faults or fractures rather than single fault planes. Further, when structures are identified in different boreholes, interpretations are made on the simplest assumptions, i.e. a planar extension in the direction of the fault planes, and identification of similar geological or hydraulic characteristics in neighbouring boreholes. However, geological structures at Äspö are known to be heterogeneous in their lateral characteristics which results in intercepts with quite varied geology, which also goes for hydraulic behaviour.

It is of course possible to classify these structures on other characteristics such as transmissivity, structural width or degree of reliability etc. However, it is believed that structure type tells more of what can be expected of the structure as regards to other behaviours (c.f. hydraulic flow, size, extent) than do other parameters.

Table 2-1 Structural classification

Fracture	Intercept of fractures without apparent shear or slip marks on fracture surfaces. Non existent ductile precursor. No cohesive or un-cohesive structures.
Fault	Visible shear or slip marks. Ductile precursor. Cohesive or un-cohesive structures.
Swarm	A large number of discontinuities that does not occur densely enough to qualify for the Zone concept. No crush in the drill core.
Zone	Intercept that occur as a large number of open faults and fractures over a short distance in the BIPS log, and as crush in the drill core. Heavily altered and deformed rock.

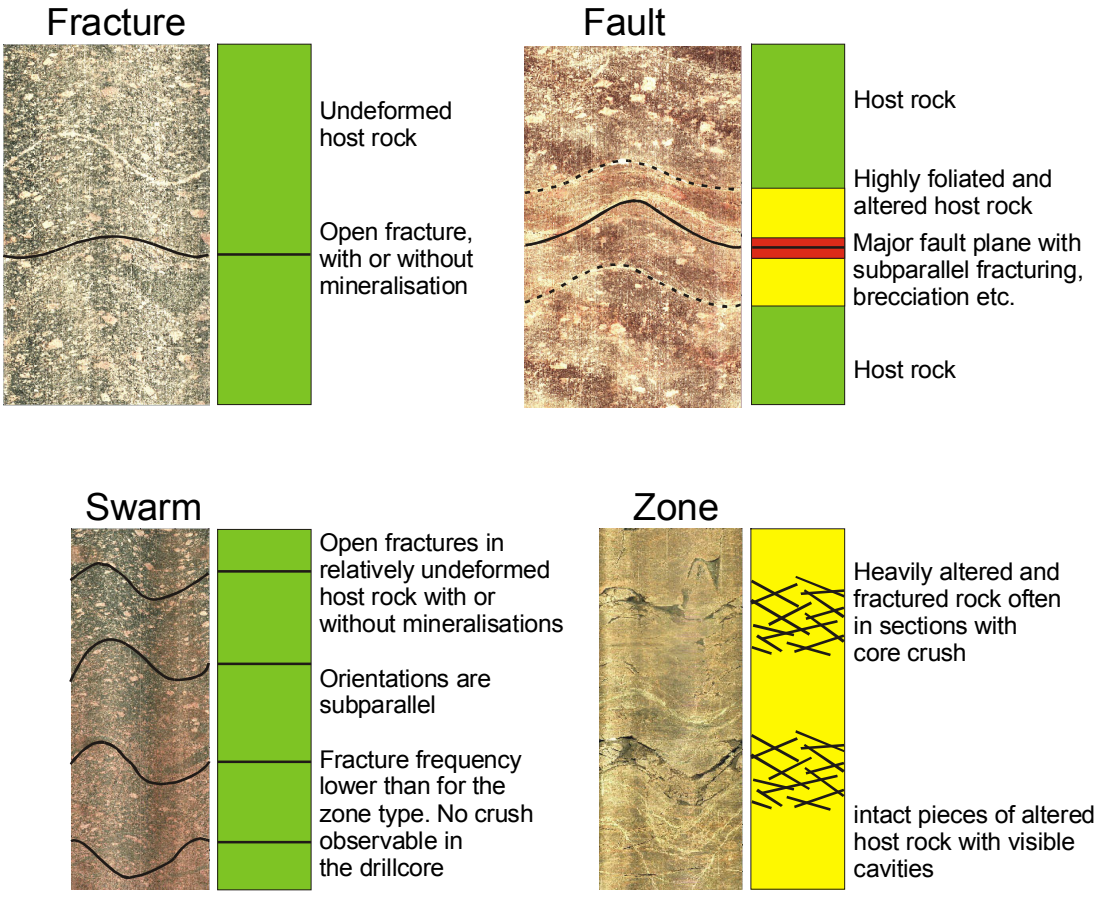

Figure 2-1 *Examples of the identified types of geological structures A) fractures, B) faults and C) swarms, D) zones.*

Below follows short descriptions of the interpreted structures in Table 2-2;

1. **Fracture**
   This structure appears as an open fracture at L=12.5 m in KA2563A. A magnitude 1U radar reflector is interpreted to intersect KA2563A at L=11.9 m. Large steep water-bearing fractures in the TBM tunnel sections around 2600 m, and in the F-tunnel coincide with a planar interpolation of this feature trending 335/82. The average width is estimated to 1 cm on the single intercept in KA2563A.

2. **Fracture-Zone**
   A fairly steep structure (109/89) associated with fractured and oxidised core at L=11.1 m, and at L=12.3 m in KA3510A (large open fracture with cavities). Similar geology is found also in KA2563A at L=68.5 m. A water-bearing fault at tunnel section L=2511 m is sub-parallel to this structure. The fracturing in the core section of Ka2563A is characterised by a network of fractures with cavities and epidotized fillings. The average width of the structure is estimated to 82 cm.

3. **Zone**
   A steep sub-parallel structure to no. 2 (110/81) intersecting KA3510A at L=37.5 m and KA2563A at L= 68.5 m. Both intercepts are characterised by severe fracturing and faulting, brecciation and core crush (zone). There are radar indications in both cores. The width varies between 220 - 40 cm in KA2563A and KA3510A, respectively.

4. **Fracture-Fault**
   This feature, trending 302/82, intersects KA2563A at L= ca 94 m and is associated with an inflow of around 40 l/min. A possible intercept of this structure is located at L=12.9 m in KA3510A. The intercept in KA2563A is characterised by oxidised and altered host rock with calcite filled fractures with cavities. A planar interpolation of structure 4 to KA2511A returns an intercept at L= ca 23 m where the rock show similar geological characteristics as in KA2563A. The section 23.08-26.6 has a recorded inflow of 30 l/min. If structure 4 is extended to intersect KA2511A, it is interpreted to intersect Structure 5 somewhere between KA2563A and KA2511A. Hydraulic responses from both drilling records and from the recently performed interference tests support that structures 4 and 5 are hydraulically coupled. The structure seem to be fairly consistent in width in all intercepts and has an average width of ca 10 cm.

5. **Fracture-Fault**
   A structure associated with large inflows in both KA3510A, KA2563A, KI0025F and KI0023B. Interpreted to intersect at L=47.7 m in KA3510A, at L=102-103 m in KA2563A, at L = 4.9 m in KI0025F and at L=7.2 m in KI0023B. The extreme inflow in KA2563A at L = 103 m (700 l/min) occur through a fault with 0.5-1 cm calcite and possible lithified gouge filling which is partly eroded. The fault has no clearly visible ductile precursor and occurs in diorite with no signs (such as decrease in grain size or chemical

dissolution of minerals) of previous tectonic events. The feature consists of a smaller fracture ending at an almost orthogonal angle to the fault and could be interpreted as a splay fracture. A fair bit of displacement has occurred along the fault plane as opposite sides match badly.

This structure seem to consist of one or a few major inter-linked fracture planes with rather thick (mm to cm) calcite filling, at times with idiomorphic crystals giving the structure a high porosity. The planar extent (113/90) is striking as the structure is identified over a distance of at least 50 m and show more or less the same orientation. The connection to KA2511A is interpreted to occur through structure 4. Hydraulic responses is observed in the innermost section of KA2512A. Geologically this section contains subparallel fracturing to both structures 5 and 4.

6. **Frac-Fault**
   This structure is associated with inflow points in KA2563A at L=153.4 m (100 l/min), in KI0025F at L=76.6 m and possibly also in KA3510A at ca 57 m. A planar projection of structure 6, trending 155/87, intersects KA2511A at ca 100 m where there is exists one open fracture with subparallel orientation (340/71). In support of BIPS observations, a radar reflector in KA2511A at L=ca 100 m is interpreted as the same structure. The structure may also interact with KA3510 through Structure 5, or a sub-parallel structure to Structure 5, intersecting at L=47.1 m in KA3510A where a fine-grained granite is intersected by 2-3 sub-parallel faults with idiomorphic calcite fillings (140/82). At L= 152-154 m in KA2563A there is 10 to 15 faults with parts of the core crushed (300/80). Fault surfaces are covered by chlorite, and possibly at a few places by lithified fault gouge, in a host rock of dark diorite with increased (sub-parallel?) foliation.

   In KI0025F the intercept is less significant and consists of a group of oxidised faults with calcite and epidote fillings. The host rock is dark diorite, but the section around the faults is reddened granite. The geological characteristics of the intercept in KI0023B is similar to KI0025F. Radar reflectors are observed at L= 44 m as well as a seismic reflector at L=40 m. Both are attributed to structure 6 (or structure 7). However, the nature of this structure makes any extensions over larger distances difficult. This structure is now interpreted to intersect at least four boreholes, but the non-unique geological character of the structure makes the interpretation not well defined. The width varies between less than a cm in KA2511A to 140 cm of faults in KA2563A.

7. **Fracture-Fault**
   Interpreted to be a steep structure, trending 120/84, intersecting KA2563A at the inflow point yielding 100 l/min inflow at L= ca 153 m (as do structure 6), KI0025FA at L= 43.5 m and KI0023B at L= 42.2 m. Radar reflectors support this structure in KI0025F at L= 43 m, KA2563A at L=151 and in KI0023B at L= 40 m. All intercepts are associated with altered oxidised diorite and fracturing. The structure can also be interpreted to intersect KA2511A at L= ca 52 m. Three intercepts are associated with inflow points;

100 l/min in KA2563A, 9 l/min in KI0025F and 6 l/min in KA2511A. The average width is ranging from less than a cm in KA2511A to 140 cm in KA2563A (at the same location as structure 6).

8. **Fault-Zone**
   This steeply dipping structure is interpreted to intersect the TBM tunnel, the F-tunnel, KA3510A and KA2563A. However, its angle in relation to KA2563A makes it difficult to determine the exact intersection point. Steep faults in the F- tunnel and in the TBM tunnel are well traced to KA3510A from 15.5 m up to 17.4 m in highly foliated, oxidised and altered diorite. The structure is interpreted to intersect KA2563A at around L=220-250 m. The specific intercept seems to be distributed over a larger distance consisting of foliated and altered diorite with a group of faults filled with epidote and calcite. Radar reflectors are interpreted in both KA3510A and KA2563A. As the intercept is more intense in KA3510A, the structure is either diverting into several smaller fault structures or diminishing beyond KA2563A. The average width is 50 cm although its total width in KA2563A may be in the order of several metres if it diverts into smaller branches.

9. **Fracture-Fault**
   This structure is currently interpreted to intersect KA2563A and KI0023B and consist of a of an open fault in KA2563A at L = ca 266 m and as a smaller fracture at L=71 m in KI0023B. Both intercepts seem to be well connected internally and with structures 20 and 13. The geological characteristics in conjunction with hydraulic responses suggests that this structure may blend in to structure 20 and possibly also with structure 13 with several splay fractures. The fault character seem to diminish towards NE and it is probably not hydraulically connected to structure 6. The width of the intercept is on average 86 cm.

10. **Fracture-Fault-Zone**
    Both radar and seismics in boreholes KA2563A, KA2511A and in KI0023B support the current interpretation of structure 10. This is a variable structure appearing as a zone in one intercept in KI0023B, single faults and fractures in KA2563A and KA2511A, respectively. The orientation of the radar reflector in KA2511A (111/85) is consistent in orientation with the crosshole seismic reflector in KA2563A (115/79). Fractured fine-grained granite dominate in KA2511A whereas greenstone is also present in the other intercepts. Fracturing is more intense in the contact between the fine-grained granite and the greenstone. The intercept in KI0023B exhibit a zone like characteristic and dominates the width of the structure which varies between less than a cm in KA2511A to 30 cm in KI0023B.

11. **Fault**
    This structure is indicated by crosshole seismic and radar in KA2511A at L=259 m. Indications in KA2563A consist of a steep and a sub-horizontal open fault in diorite. Current interpretation of orientation is 288/88. The width is approximately 15 cm, but may vary as it is picked up by crosshole

seismics. It has not been tested in any hydraulic test program and little is known of its connectivity.

12. **Unknown type**
A seismic reflector beyond the limit of all boreholes is interpreted as being a possible boundary zone as proposed by the previous block scale siting investigation. Orientation is 355/90.

13. **Fault**
Structure 13 has been identified in borehole KI0023B at L=85.6 m and in KA2563A at L=207 m. It is featured as a distinct fault, about 15-20 cm wide with the average orientation of 142/86. The structure is parallel to the interpreted Structure 20, and is assumed to be of similar extension. It is well connected to structures 20 and 9 (Andersson et al 1998).

15. **Fault**
A radar reflector and a number of faults in KA3510A describe this structure. At 117.90-120.89 m, 15 faults intersect KA3510A in fine-grained granite. There is a cm wide sub-parallel calcite filled fracture in the middle of this group, although it is sealed in the drill core, it may well be conductive in more porous sections outside the borehole. It seem possible that these fractures take part in the measured slow increase in inflow as registered during drilling of this borehole. Structure 15 is indicated by hydraulic responses in the innermost sections of KA3573A and is also supported by radar reflectors in the same section. Preliminary results from interference tests indicate that structure 15 may be in contact with several other structures, in particular structure 7 and possibly also structure 6. Orientation is interpreted to 268/88.

16. **Zone**
Evidence for a gently dipping fine-grained granite body intersecting KA2563A at L= ca 56 m and associated with a greenstone and massive faulting and core crush in KA2511A at L = 104-105 m. This structure is also supported by a seismic crosshole reflector and the orientation of the sub-horizontal rock contacts in both KA2563A and in KA2511A**.** The structure can be described as a fractured lithological body with variable thickness, extent and degree of fracturing rather than a traditional zone. However Structure 16 may be an important hydraulic connector between steep NW trending zones. The orientation is estimated to 177/18 and the average width to 110 cm.

17. **Fracture**
This structure is also most probably a gently dipping fine-grained granite associated with greenstone in KA2563A at L=109 m, and with an intensely deformed fine-grained granite in KA2511A at L= 133 m. However its structural impact occur as a fracture in the contact or in the fine-grained granite. The lithological body is interpreted to follow a gently dipping cross-hole seismic reflector intersecting KA2563A at L=110.5 m and KA2511A at L=125 m. Previous seismic investigations in KA2511A also show a gently

dipping reflector at this depth. There are also several sub-horizontal faults in KA2511A, in section L = 130 - 132 m, associated with altered diorite and fine-grained granite, calcite and epidote fillings. This structure is geologically more prominent than zone 16, but is not necessarily a conductive structure as the deformation (in KA2511A) is ductile and not brittle. Sub-horizontal structures are interpreted to act as hydraulic connectors, but seem to show a very heterogeneous conductive character. The orientation is estimated to 245/05 and the average width to 190 cm.

18. **Fracture-Swarm-Fault**
The last identified gently dipping fine-grained granite structure is supported by both radar and seismic in KA2563A and KA2511A. It is currently interpreted to be a dry intercept even if there exist a 20 l/min inflow in KA2511A which is measured in the interval up to L=242 m. However, as this structure intersects at L=242.5 m the inflow is not interpreted to be associated with this structure but rather to a steep structure at L=240.5 m (Structure 10). Inspection of the core shows a fault crush with a parallel epidotized fault in KA2511A. The main fault has chlorite and some calcite fillings and occurs in fine-grained granite (close to the contact with the diorite). The host rock in this core section (25 cm) is influenced by hydro-thermal activities In KA2563A it occurs at L= 109 m with a similar geological signature. This structure is also strengthened by a radar reflector in KA2563A at L=191 m and a seismic reflector in KA2511A at L=240 m. The width is estimated to 20 cm and the orientation is 024/16. Further, it is also identified as a fracture swarm in KI0023B at L=75.5 m, supported by radar and seismic evidence. However, the performed interference test program by Andersson et al (1998) show, in a test in KA2563A that there exist no connectivity in structure 18.

19. **Fracture-Fault-Zone**
Structure 19 is identified in the BIPS log in four boreholes, KA2563A at L = 227 m, KI0025F at L = 166 m, KA2511A at L = 198 m and in KI0023B at L=112 m. A larger inflow is noted in KI0025F (30 l/min). However, the zone is interpreted to be heterogeneous in its structure, with a non-conductive intercept in KA2511A. The orientation is 335/61. This structure is characterized as a fault or network of faults in fine grained granite, alternatively in diorite with a rim of alteration around the fault plane. The width is variable and is observed between 10 to 35 cm. Hydraulic tests suggests that it is less transmissive at ligher levels in the block. This is confirmed by the geological characteristics which show a more zone like type in lower levels in SE, and fault type in the higher levels in NW.

20. **Fracture-Swarm-Fault**
Structure 20 is found in KA2563A at L = 188.7 m as a group of faults with observable apertures on the BIPS log, and in KA2511A at L= 122 m. When drilling KI0025F, at L = 87.7 a single response was measured in KA2563A. Similar hydraulic responses, and later also interference tests, confirm and extend this structure also to KI0023B at L=69.8 m. The geological characteristics are not as dramatic in KI0025F, KI0023B and in KA2511A

as in KA2563A. In the latter boreholes, this structure is identified as an open fracture or a group of open fractures in altered diorite. No registration was made in KA2511A at the time of drilling into L= 87.7 m in KI0025F. Structure 13 and structure 20 has similar geological characteristics and may well be connected through some splay fractures. The orientations of the fractures are similar in all intercepts, giving this structure an interpreted orientation of 318/84.The average width is estimated to 100 cm emphasizing that this structure most likely consists of a group of interconnected fractures and faults.

Z. **Zone**

The Z structure is a large zone, unlike all other structures found in the drilled boreholes in the TRUE Block Scale experiment as regards to its geological characteristics. This structure is identified by a large section of core crush from L = 188 m to the end of the borehole which is also confirmed by the BIPS image. During the drilling it was featured by successively increased inflow and mobilisation of unconsolidated material. A mineralogical analysis performed by Tullborg (1998) show that the characteristics of this zone is similar to the characteristics of Zone NE-1, with brecciated, crushed and faulted rock with large portions of altered host rock, (diorite and fine grained granite). The contents of fault gouge in the analysed sample was low, possibly due to that gouge may have been flushed out during drilling and uptake of the core. Geometrically, this zone is sub-parallel to NE-2, EW-3 and NE-1. However, based on the conceptual model of the site scale zones (Rhén, 1997), zone NE-1 is located over 80 m south of the Z structure, and EW-3 is approximately 30 m south of the Z structure. However, zones NE-2, EW-3 and NE-1 are not well identified in this particular part of the HRL. Splay structures and minor branches to these major zones may therefore exist. It is interpreted that the Z structure is such a branch of either EW-3 or NE-1. The characteristics of zone NE-2 is completely different, dominated by mylonites, and a few conductive faults.

NE-2 This zone is NE-2 and data for this zone can be obtained from Rhén et al (1997). No intercepts in this zone have been identified in the TRUE Block Scale set of boreholes.

EW-1 This zone is EW-1 and data for this zone can be obtained Rhén et al (1997).

EW-3 occur as a zone deviating westwards from NE-1. Data for this zone can be obtained from Rhén et al (1997).

Table 2-2 Summary of identified structures in the TRUE Block Scale volume.

	KA2563A				KA2511A				KA3510A				KI0025F				KI0023B				Width	Geology
Structures	Depth (m)	Width (cm)	Type	Strike/ dip	Depth (m)	Width (cm)	Type	Strike/ dip	Depth (m)	Width (cm)	Type	Strike/ dip	Depth (m)	Width (cm)	Type	Strike/ dip	Depth (m)	Width (cm)	Type	Strike/ dip	Average width	geological description
1	12.5	0.2	Frac	335/82																	1	Fgranite, fractured, faults, faults in the tunnel
2	68.5	220	Zone	135/87					11.1	15	Frac	309/75									110	Oxidized, fractured, crush
3	68.5	220	Zone	135/87					37.5	40	Zone	106/81									130	Oxidized, fractured, crush
4	94.4	6	Frac	296/74	23.1	10	Frac	300/80	12.9	8	Fault	115/89									10	Fgranite, greenstone, crush
5	103	2	Frac	114/89					47.7	10	Fault	138/75	4.9	10	Frac	307/57	7.2	5	Frac	112/87	10	Variable structure partly altered
6	153.4	140	Fault	111/73	100	0.2	Frac	340/71	56.7	0.5	Frac	131/87	76.6	80	Frac	107/65	44.2	10	Fault	103/87	50	oxidized network with faults
7	153.4	140	Fault	111/73	52.4	0.2	Frac	119/79					43.5	25	Frac	253/84	42.2	4	Frac	338/83	40	Oxidized, fractured, crush
8	242.4	8	Fault	026/84					16.1	100	Zone	232/89									50	Faultzone structure in TBM tunnel and KA3510, KA2563A
9	265.8	5	Fault	096/85													71.1	10	Frac	123/86	8	Oxidized, single open faults
10	351.3	25	Fault	124/80		0.5	Frac	127/85									171	30	Zone	298/83	20	Variable structure partly in greenstone
11					258	15	Fault	288/88													10	Visible as single fault in diorite
12																						Only observed by seismics, see Table XXX
13	207	20	Fault	321/86													85.6	15	Fault	318/89	17	Fault with altered and deformed diorite
15									118	60	Fault	269/88									60	Fgranite, crush (118-119 m in KA3510A)
16	56.3	120	Zone	011/40	105	100	Zone	233/18													110	Fgrained granite, oxidized
17	108.9	0.2 (140) 0.1	Frac	222/34	132	5 (230)	Frac	270/16													3 (190)	Fgrained granite, greenstone
18	194.3	(20)	Frac	012/18	243	10	Fault	155/9									75.5	80	Swarm	348/41	20	Fgrained granite
19	226.8	10	Fault	308/47	198	35	Frac	324/87					166.4	65	Zone	338/74	112	20	Fault	342/87	30	Faults in Finegrained granite, alteration
20	188.7	5 (60)	Fault	316/82	122	0.2 (100)	Frac/ Swarm	336/67					87.7	0.2	Frac	336/77	69.8	20	Fault	157/82	100	Open fault KA2563A, other intercepts faultgroups in altered diorite
Z													192.1	+550	Zone	243/77					+550	Minor branch of either EW-3 or NE-1

Table 2-3 Identified structures in KA2563A with geophysical and hydraulic indications.

KA2563A											
Structures	Depth	Width	Type	Orientation	Radar			Sesmics			Inflow	Observed in interference test program
	(m)	(cm)		(deg °)	(m)	ori (°)	M	l^2	(m)	ori (°)	l/min	Test[3]
1	12.5	0.2	Frac	335/82	12		1U					
2	68.5	220	Fault	135/87	69	166/79	1U					
3	68.5	220	Zone	135/87	70	166/80	1U					
4	94.4	6	Frac	296/74	95	258/54	1U				35-40	X
5	103	2	Frac	114/89	100	053/23	2				700	X
6	153.4	140	Fault	111/73	151	123/76	1				100	
7	153.4	140	Fault	111/73	151	123/76	1				100	X
8	242.4	8	Fault	026/84	244	041/74	2U					
9	265.8	5	Fault	096/85				A	269	264/83		X
10	351.3	25	Fault	124/80	349	115/79	1U					X
11												
12												
13	207	20	Fault	321/86	207	139/58	1					X
15												
16	56.3	120	Zone	011/40	53	062/43	1U					
17	108.9	0.2 (140)	Frac	222/34								
18	194.3	0.1 (20)	Frac	012/18	191	220/18[1]	1					
19	226.8	10	Fault	308/47								X
20	188.7	5 (60)	Fault	316/82	191	167/76[1]	1					X
Z												

[1]the same reflector with two different interpretations of the orientation. See Carlsten (1996)

[2] A corresponds to investigations by Heikkinen et al (1997) and B to Cosma et al (1998), respectively.

[3]The interference test results are explained in Andersson et al (1998)

Table 2-4 Identified structures in KA2511A with geophysical and hydraulic indications

KA2511A											
Structures	Depth	Width	Type	Strike/ dip	Radar			Sesmics			Inflow	Observed in interference test program
	(m)	(cm)		(deg °)	(m)	ori (°)	M	l^2	(m)	ori (°)	l/min	Test[3]
1												
2												
3												
4	23.1	10	Frac	300/80				B	2	109/85		
5								B	-6	109/85		
6	100.1	0.2	Frac	340/71				A	104	128/66		
7	52.4	0.2	Frac	119/79								X
8												
9												
10	240.5	0.5	Frac	127/85	241	111/85	1					X
11	258.2	15	Fault	288/88	259	340/69	U					
12				355/90				A	378	175/73		
13												
15												
16	104.7	100	Zone	233/18							60	X
17	132.4	5 (230)	Frac	270/16	136	169/11	1					X
18	242.5	10	Fault	155/9				A	240	204/17		X
19	198.2	35	Frac	324/87	199	112/68	2					X
20	122	0.2 (100)	Frac/ Swarm	336/67	121	248/71	2					X
Z												

[2] A corresponds to Heikkinen et al (1997) and B to Cosma et al (1998), respectively.

[3]The interference test results are explained in Andersson et al (1998)

Table 2-5 Identified structures in KA3510A with geophysical and hydraulic indications

KA3510A								
Structures	Depth	Width	Type	Strike/ dip	Radar			Inflow	Observed in interference test program
	(m)	(cm)		(deg °)	(m)	ori (°)	M	l/min	Test[3]
1									
2	11.1	15	Frac	309/75	13	292/90	1U		
3	37.5	40	Zone	106/81	37	107/87	1U		
4	12.9	8	Fault	115/89	13	292/90	1U		
5	47.7	10	Fault	138/75	47	123/88	1U	70	X
6	56.7	0.5	Frac	131/87					
7									
8	16.1	100	Zone	232/89					
9									
10									
11									
12									
13									
15	118	60	Fault	269/88	117	274/80	3	40	X
16									
17									
18									
19									
20									
Z									

[3]The interference test results are explained in Andersson et al (1998)

Table 2-6 Identified structures in KI0025F with geophysical and hydraulic indications

KI0025F								
Structures	Depth	Width	Type	Strike/ dip	Radar			Inflow	Observed in interference test program
	(m)	(cm)		(deg °)	(m)	ori (°)	M	l/min	Test[3]
1									
2									
3									
4									
5	4.9	10	Frac	307/57	3	315/75	1U	40	X
6	76.6	80	Frac	107/65					
7	43.5	25	Frac	253/84	43	210/64	1U	9	X
8									
9									
10									
11									
12									
13									
15									
16									
17									
18									
19	166.4	65	Zone	338/74	166	331/55	3	28	X
20	87.7	0.2	Frac	336/77	86	081/36	1U		X
Z	192.1	+550	Zone	243/77	192	277/71	1U	38	X

[3]The interference test results are explained in Andersson et al (1998)

Table 2-7 Identified structures in KI0023B with geophysical and hydraulic indications

KI0023B								
Structures	Depth	Width	Type	Strike/ dip	Radar	Sesmics	Inflow	Observed in interference test program
	(m)	(cm)		(deg °)	(m) ori (°) M	I[1] (m) ori (°)	l/min	Test[3]
1								
2								
3								
4								
5	7.2	5	Frac	112/87	7.3 152/43 -[2]			X
6	44.2	10	Fault	338/83	44 140/64 -[2]	B 40 110/90	48	X
7	42.2	4	Frac	103/87	33 085/89 -[2]		2	
8								
9								
10	170.7	30	Zone	298/83	170 304/73 -[2]	B 170 294/78	18	X
11								
12								
13	85.6	15	Fault	318/89				X
15								
16								
17								
18	75.5	80	Swarm	348/41	74 138/42 2	B 68 300/07		X
19	111.6	20	Fault	342/87				X
20	69.8	20	Fault	157/82	70 350/57 -[2]	B 68 110/90	3	X
Z								

[1] A corresponds to investigations by Heikkinen et al (1997) and B to Cosma et al (1998), respectively.

[2] no record (Carlsten 1998).

[3] The interference test results are explained in Andersson et al (1998)

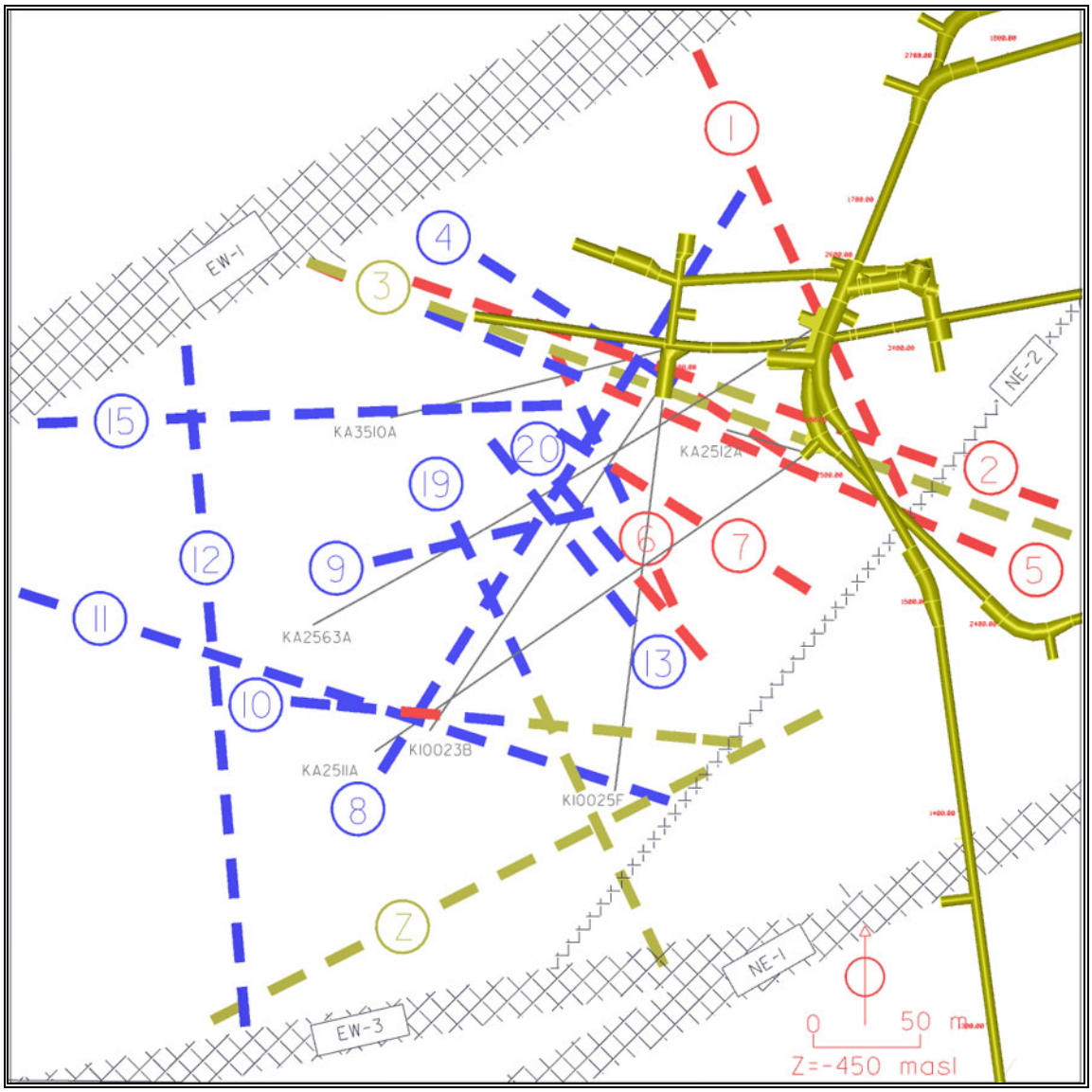

Figure 2-2 *Structural geological model of the TRUE Block Scale volume. The identified structures are coloured according to the geological signature, where fracture is represented by red, fault by blue, swarm by green, and zone by yellow. Hatched gray areas represent site scale zones from Rhén et al. (1997). See text for detailed explanations of the model.*

3. Complementary information to the structural geological model from performed interference tests

As described by Andersson et al (1998) in the evaluation of interference tests in the TRUE Block Scale volume, the test results show that major responses can be divided into two types of response characteristics, global responses (tests ENW-1, ENW.2,ESV-2, 2512A and 2598A), and pronounced local response characteristics (tests ESV-1a-ESV1c, 23BP4).

The global tests can be interpreted to be performed in steeply NW trending structures according to Andersson et al (1998), c.f. structures 5, 6 and 7. There is a good connectivity between these steeply dipping structures as can be seen in the response pattern in KA2511A. Based on the geological information this can be explained either by the steep NE trending structure 8 or by sub-horizontal structures 16 or 17. Structure 8 has no recorded increase in inflow at its most prominent borehole intercept, in KA3510A but are believed to extend all the way to KA2598A (L=45 m). Some inflow occur in its prolongation into the TBM tunnel. This indicates that structure 8 are heterogeneous and may provide connectivity in local patches. However, to provide the widespread response pattern described by Andersson et al (1998) it is considered unlikely that it is done by structure 8 alone. Structures 16 and 17 are both irregular, but may well connect steeper structures over a shorter distance.

As structure 7 is not geologically recorded to continue through KA3510A but may terminate against structure 15, there is a possibility that structure 15 helps propagate responses in the NW trending fault system of structures 4, 5, and 6. Structure 6 also continues through KA3510A and intersects structures 4 and 5 between KA3510A and KA3600F. All together, the combination of structures 15, 6, 16 and 17 with a little help from structure 8 are most likely providing the recorded connectivity between the NW trending faults.

Another result presented by Andersson et al (1998) is that structure 5 continues into KA2512A (test ENW-1). This is in accordance with the estimated planar extension of the previous structural model although no geological indications have been defined for this intercept.

The local responses have been measured primarily in structures 20 and a nearby sub parallel fault, not previously detected, now named structure 13. Based on the local response tests there are clear indications that structures 20 and 13 are in contact with each other but in limited contact with the rest of the network, except for structure 9, c.f. Figure 2-2. The geological characteristics of both these two faults are similar and does also exhibit splay fractures which will connect the two. Good responses are measured in structure 9 when pumping is performed in section L=70.95-69.95 (Andersson et al 1998). The structure in this section is not interpreted as structure 20 but rather as structure 9. Structure 9 may then possibly terminate or blend into structures 13 and 20, thus connecting to this group of sub parallel NW trending faults. This is also confirmed

by the responses from test #11 (Andersson et al 1998), where hydraulic responses between KA2563A and KI0023B are interpreted to propagate through structure 9 in connection with structures 13 and possibly also 20. This group of three structures are somewhat hydraulically separate from the rest of the block and may be suitable for a detailed investigation.

Structure 19 is confirmed by test #9 (Andersson et al, 1998). Structure 19 is well connected to structure Z but seem to be hydraulically heterogeneous as low responses are measured at intercepts in KA2511A and KA2563A. This is in good accordance with the heterogeneous geological characteristics of this structure as it ranges from fracture and fault in KA2511A and KA2563A to a 65 cm wide zone in KI0025F.

In summary, the major connectivity in the block may well be explained by the existing steeply dipping structures, with the addition of structure 13. However, there is not enough information to exclude that either sub horizontal structures 16 or 17 are acting as connectors between the steeply dipping NW trending fault system through the TRUE block. A structural conceptualisation of the geological heterogeneity of the block is given in Figure 3-1 to help understand possible complexities when making simplifications of the identified structures for other purposes, i.e numerical models. It is clear that few, if any, structures can be easily classified into one structural group. Observed heterogeneity of the hydraulic characteristics show the same pattern although structure 20, 3 and 9 forms a relatively isolated group in the centre of the block.

In Figure 3-1, the planned borehole KI0025F02 is shown between KI0025F and KI0023B. Predictions of structural intercepts has been performed prior to the drilling of this borehole and are shown in Table 3-1.

Finally, explicit extension and orientation of each and every defined structure in the TRUE Block Scale volume is given in Table 3-2 and Table 3-3 in the form of the equation of the plane and the terminations where applicable.

Table 3-1 Predicted depth of intersection and expected inflow at interpreted structures in the planned borehole KI0025F02.

Structure #	Predicted depth[1] (m)	Predicted inflow[2] (l/min)
5	5-8	<10
6	69-73	5-10
7	48-52	40-60
10	183-187	15-20
11	(238)	<10
13	123-127	<5
18	67-71	0
19	145-151	5-10
20	92-97	<5

[1]Predictions made on the basis of the Sep´98 structural model
[2]Predictions made by Anders Winberg (Aug 17) on the basis of results from KI0025F and KI0023B

Table 3-2 Equation of the plane for the defined structures in the TRUE Block Scale volume. Terminations of each structure is given where applicable.

Structures	Equation of the plane (in the form Ax+By+Cz+D=0)				Strike	Dip	Average width (cm)	Type	Terminations[1]
	A	B	C	D					
1	0.8973	0.4190	0.1388	-4806.96	335	82	1	Frac	EW-1, NE-2
2	-0.3255	-0.9454	0.0175	7500.92	109	89	110	Frac-Zone	EW-1, RW
3	-0.3352	-0.9300	0.1507	7460.11	110	81	130	Zone	EW-1, RW
4	-0.5284	-0.8363	-0.1462	7030.27	302	82	10	Frac-Fault	EW-1, #5
5	-0.3944	-0.9189	0.0080	7421.24	113	90	10	Frac-Fault	EW-1, RW
6	-0.9051	-0.4218	0.0533	4810.05	155	87	50	Frac-Fault	#5, north of #20[2]
7	0.4973	0.8613	-0.1045	-7216.54	120	84	40	Frac-Fault	#15, NE-2
8	0.7947	-0.4946	-0.3518	1886.88	212	69	50	Fault-Zone	#1, south of #10[2]
9	0.2413	-0.9679	0.0698	6526.95	76	86	8	Frac-Fault	West of #19, east of #20[2]
10	0.0916	0.9458	0.3116	-6736.41	276	72	20	Frac-Fault-Zone	#12, NE-2
11	0.3043	0.9519	0.0349	-7292.15	288	88	10	Fault	LW, NE-2
12	0.9960	0.0891	0.0000	-2371.27	355	90	-	-	EW-1, EW-3
13	0.7832	0.6179	-0.0698	-5960.09	142	86	17	Fault	south of #15, north of NE-2[2]
15	-0.0349	0.9988	0.0349	-7145.11	268	88	60	Fault	EW-1, #6
16	0.3046	0.0155	-0.9524	-1079.35	177	18	110	Zone	EW-1, NE-1, LW, RW, NW, SW
17	0.0370	-0.0791	-0.9962	86.92	245	5	3 (190)	Frac	EW-1, NE-1, LW, RW, NW, SW
18	-0.2496	0.1119	-0.9619	-782.90	24	16	20	Frac-Swarm-Fault	EW-1, NE-1, LW, RW, NW, SW
19	-0.7924	-0.3751	-0.4810	3948.95	335	61	30	Frac-Fault-Zone	north of #9, NE-1[2]
20	-0.7409	-0.6643	-0.0987	6147.39	318	84	100	Frac-Swarm-Fault	south of #15, north of NE-2[2]
Z	-0.4424	0.8682	0.2250	-5158.48	243	77	+550	Zone	EW-3, RW, LW
EW-1	0.4792	-0.8547	0.1994	5472.54	61	78		Site scale zone	see Rhén et al (1997)
EW-3	-0.1994	0.9612	-0.1908	-6409.20	78	79		Site scale zone	see Rhén et al (1997)
NE-1	-0.4380	0.8472	0.3008	-4905.35	243	72		Site scale zone	see Rhén et al (1997)
NE-2	0.7882	-0.5728	0.2249	2589.13	36	77			see Rhén et al (1997)
NNW-7	-0.9040	-0.4186	-0.0868	4915.15	113	78	Not included in Sep ´98 model		see Rhén et al (1997)
RW	1.0000	0.0000	0.0000	-2150.00	0	90		Eastern boundary	500 m block[1]
LW	1.0000	0.0000	0.0000	-1650.00	0	90		Western boundary	500 m block[1]
NW	0.0000	1.0000	0.0000	-7420.00	90	90		Northern boundary	500 m block[1]
SW	0.0000	1.0000	0.0000	-6920.00	90	90		Southern boundary	500 m block[1]

[1] based on a 500x500x500 m block centered on Äspö local coordinates 1900,7170,-450

[2] vertical termination based on Sep ´98 model at Z=-450 m, with no concern of how intersections occur with other structures at depth

Table 3-3 Co-ordinates of the Sep ´98 structural model. For explanations where each structure terminates, please see Table 4-1 and Figure 2-2.

Structures	Coordinates																	
	X_1	Y_1	Z_1	X_2	Y_2	Z_2	X_3	Y_3	Z_3	X_4	Y_4	Z_4	X_5	Y_5	Z_5	X_6	Y_6	Z_6
1	1917.85	7431.31	-200.00	2017.44	7218.04	-200.00	2120.33	7163.29	-700.00	2022.30	7373.21	-700.00						
2	1739.92	7331.54	-200.00	2150.00	7190.34	-200.00	2150.00	7181.11	-700.00	1858.63	7281.44	-700.00						
3	1772.92	7350.05	-200.00	2150.00	7214.16	-200.00	2150.00	7133.13	-700.00	1811.62	7255.08	-700.00						
4	1748.48	7336.35	-200.00	1809.35	7297.90	-200.00	2262.36	7099.12	-700.00	1919.63	7315.64	-700.00						
5	1736.03	7329.37	-200.00	2150.00	7151.68	-200.00	2150.00	7147.35	-700.00	1849.52	7276.33	-700.00						
6	1924.49	7248.48	-200.00	1966.95	7157.36	-200.00	1942.71	7146.24	-700.00	1890.23	7258.85	-700.00						
7	1949.72	7228.90	-200.00	2002.98	7198.15	-200.00	2072.43	7097.37	-700.00	1822.08	7241.91	-700.00						
8	2022.61	7206.95	-200.00	1902.16	7013.42	-200.00	1742.64	7112.71	-700.00	1971.92	7481.11	-700.00						
9	1923.23	7208.26	-200.00	1785.35	7173.88	-200.00	1793.65	7139.91	-700.00	1931.54	7174.29	-700.00						
10	1752.97	7018.55	-200.00	1864.61	7007.73	-200.00	2109.73	7148.70	-700.00	1738.10	7184.71	-700.00						
11	1650.00	7140.22	-200.00	1902.28	7059.57	-200.00	2028.88	7037.43	-700.00	1650.00	7158.55	-700.00						
12	1725.68	7323.56	-200.00	1755.28	6992.63	-200.00	1764.00	6895.17	-700.00	1735.62	7212.47	-700.00						
13	1890.70	7226.80	-200.00	1976.41	7118.17	-200.00	1948.87	7096.62	-700.00	1863.16	7205.25	-700.00						
15	1530.74	7214.26	-200.00	1933.87	7228.34	-200.00	1896.91	7244.52	-700.00	1785.88	7240.64	-700.00						
16	1901.15	6920.00	-412.81	1650.00	6920.00	-493.14	1650.00	7213.85	-488.36	1973.26	7420.00	-381.62	2150.00	7420.00	-325.09	2150.00	7019.84	-331.60
17	1650.00	6919.29	-401.13	1650.00	7370.48	-436.97	1741.87	7420.55	-437.54	2150.00	7420.55	-422.39	2150.00	7041.67	-392.29	1946.49	6919.29	-390.13
18	1650.00	6919.19	-437.07	1650.00	7234.37	-400.40	2012.12	7420.53	-472.70	2150.00	7420.53	-508.48	2150.00	7096.04	-546.23	1847.71	6919.19	-488.37
19	1719.55	7151.51	-200.00	1872.04	6829.40	-200.00	2048.38	7098.09	-700.00	1967.67	7268.59	-700.00						
20	1863.33	7205.20	-200.00	1955.89	7101.98	-200.00	1994.81	7132.87	-700.00	1902.25	7236.09	-700.00						
Z	1737.23	6941.12	-440.61	2101.77	7064.51	-200.00	2150.00	7218.64	-700.00	1650.00	6963.88	-700.00	1650.00	6963.88	-700.00			

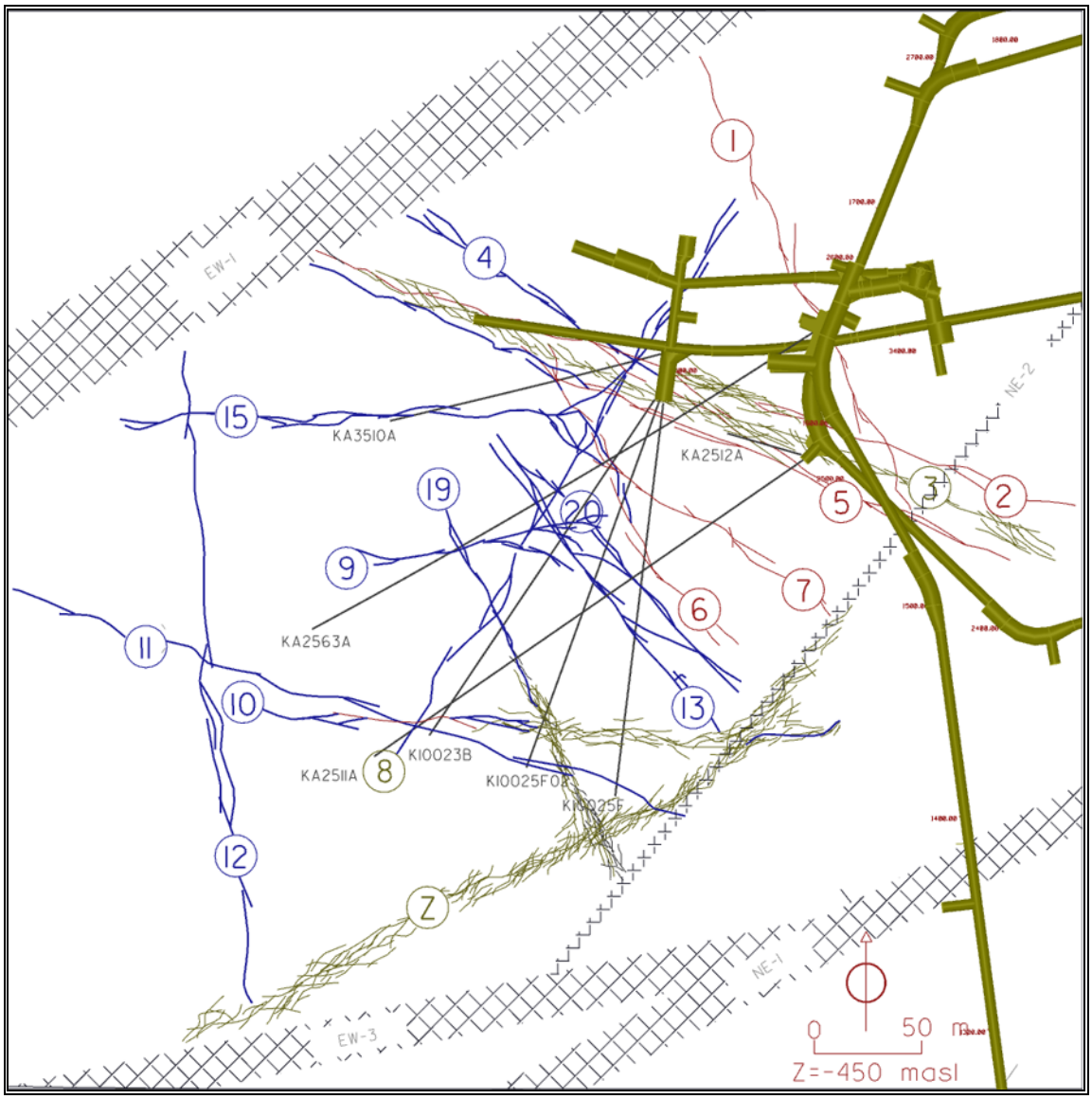

Figure 3-1 *Structural geological conceptualisation of the TRUE block. Colours refer to the same geological classification as in Figure 2-2, where red represent fracture, blue faults and yellow zones. Fracture swarms exist but are limited in extent, c.f. Table 2-1. Note the planned borehole KI0025F02.*

4. References

Andersson, P, Ludvigsson, J-E, Wass, E., (in prep) : True Block Scale Project, preliminary characterization stage. Combined interference tests and tracer tests. Performance and preliminary evaluation. Äspö Hard Rock Laboratory, International Progress Report IPR-01-44.

Carlsten, S. 1996a : Results from borehole radar measurement in KA2563A. Swedish Nuclear Fuel and Waste Management Company, Internal Report.

Carlsten, S. 1996b : Results from borehole radar measurement in KA3510A. Swedish Nuclear Fuel and Waste Management Company, Internal Report.

Carlsten, S. 1997 : Results from borehole radar measurement in KI0025F. Swedish Nuclear Fuel and Waste Management Company, Internal Report.

Carlsten, S. 1998 : Results from borehole radar measurement in KI0023B. Swedish Nuclear Fuel and Waste Management Company, Internal Report.

Cosma, C., Enescu, N., Heikkinen, P., Keskinen, J., 1998 : Seismic Investigations in KI0023B and integrated interpretation of results from the VSP and HSP measurements between KA2511A and KA2563A (1997) and the VSP measurements in KA2511A (1994. Swedish Nuclear Fuel and Waste Management Company, Internal Report.

Gentzschein, B., Nilsson, G., 1996: Compilation of activities and events during drilling of KA2563A and KA3510A. Swedish Nuclear Fuel and Waste Management Company, Internal Report.

Gentzschein, B., 1996: Pressure build-up tests performed prior to cement grouting carried out during drilling of borehole KA2563A. Swedish Nuclear Fuel and Waste Management Company, Internal Report.

Gentzschein, B. and Nilsson, G. 1997 : Compilation of activities and events during drilling of KA2563A and KA3510A. Swedish Nuclear Fuel and Waste Management Company, Internal Report.

Gentzschein, B., 1997 : Detailed flow logging of core borehole KA2563A. Swedish Nuclear Fuel and Waste Management Company, Internal Report.

Gentzschein, B., 1997 : Detailed flow logging of core boreholes KA2511A, KI0025F and KA3510A using a double packer system. Swedish Nuclear Fuel and Waste Management Company, Internal Report.

Hermanson, J., Follin S, 1997 : TRUE Block Scale Project. Update of the structural model using characterisation data from KI0025F. Swedish Nuclear Fuel and Waste Management Company, Internal Report.

Heikkinen, P. and Keskinen, J. 1997 : Crosshole seismic investigation in boreholes KA2563A and KA2511A. Swedish Nuclear Fuel and Waste Management Company, Internal Report.

Nilsson, G., 1996 : Compilation of data from cement grouting during drilling of KA2563A and KA3510A. Swedish Nuclear Fuel and Waste Management Company, Internal Report.

Nilsson, G. 1998 : Compilation of activities and events during drilling of KI0023B.. Swedish Nuclear Fuel and Waste Management Company, Internal Report.

Nilsson, G., 1998 : Boremap logging of core from borehole KI0023B. Swedish Nuclear Fule and Waste Management Company, Internal Report.

Olsson, O. (ed) 1994 : Localisation of experimental sites and layout of turn 2 - results from core mapping, radar and hydraulic investigations. Compilation of technical notes., Äspö Hard Rock Laboratory, Progress Report PR 25-94-15. Swedish Nuclear Fuel and Waste Management Company.

Rhén,I, Gustafson, G., Stanfors, R., Wikberg, P. Geoscientific evaluation 1997/5 (in press) : Models based on site characterisation 1986-1995 1997. SKB Technical Report, TR 97-06. Swedish Nuclear Fuel and Waste Management Company.

Stråhle, A. 1997 : Interpretation of BIPS images of boreholes KA2563A and KA3510A. Swedish Nuclear Fuel and Waste Management Company, Internal Report.

Stråhle, A., 1998 : Borehole TV images of borehole KA2511A. Swedish Nuclear Fuel and Waste Management Company, Internal Report.

Stråhle, A., 1998 : Borehole TV images of borehole KI0025F. Swedish Nuclear Fuel and Waste Management Company, Internal Report.

Winberg, A., 1997 : Pressure responses due to drilling of KI0025F. Swedish Nuclear Fuel and Waste Management Company, Internal Report.

Talbot, C. J., 1990 : Some clarification of the tectonics of Äspö and its surroundings. Swedish Nuclear Fuel and Waste Management Company, Äspö Hard Rock Laboratory, Progress Report PR 25-90-15.

Tullborg, E-L., (in prep) : Mineralogical and geochemical characterisation of samples taken from borehole KI0025F: (zone Z), and KA2563A and KA3573A (structure 5). Swedish Nuclear Fuel and Waste Management Company, Internal Report.

APPENDIX 1

Database of major structures in boreholes KA2563A, KA2511A, KA3510A, KI0025F and KI0023B

KA2511A

Location (m)	Width (cm)	Type	Rocktype/ Grout	Strike	Dip	Inflow (l/min)	Associated Structure
19.9	0.2	Fracture	Aplite	308	80		
23.1	10	Fracture	Grout	300	80		4
26.2	0.2	Fracture	Äspödiorite	308	17		
30.3	0.2	Fracture	Äspödiorite	323	81		
38.9	0.2	Fracture	Äspödiorite	143	87		
40.1	5	Fault	Äspödiorite	6	78		
46.2	0.2	Fracture	Äspödiorite	4	38		
52.4	0.2	Fracture	Äspödiorite	119	79	51.2	7
57.7	2	Fracture	Aplite	236	51	0.4	
59.5	45	Fracture	Äspödiorite	319	86		
76.4	10	Fracture	Äspödiorite	42	15		
76.8	0.2	Fracture	Äspödiorite	4	90		
92.3	0.2	Fracture	Äspödiorite	297	29		
100.1	0.2	Fracture	Äspödiorite	340	71	10	6
104.7	100	Zone	Äspödiorite	233	18	11.3	16
106.7	60	Fault	Aplite	267	31		
109	0.5	Fracture	Äspödiorite	114	87		
120.2	5	Fault	Äspödiorite	10	83		
121.1	0.2	Fracture	Äspödiorite	352	26		
122	0.2	Fracture	Äspödiorite	321	73		20
122.8	100	Swarm	Aplite	336	67		---::---
132	0.5	Fracture	Aplite	349	48		
132.4	5	Fracture	Aplite	270	16		17
132.8	230	Fracture	Aplite	349	48		---::---
142.9	10	Fracture	Äspödiorite	30	73	4	
148.4	10	Fracture	Äspödiorite	19	62		
150	5	Fracture	Äspödiorite	240	17		
151.3	7	Fracture	Äspödiorite	0	77	0.5	
155.4	10	Fracture	Äspödiorite	233	34		
156.2	0.2	Fracture	Äspödiorite	232	46		
158.7	10	Fault	Äspödiorite	249	73		
162.6	0.2	Fracture	Äspödiorite	324	54		
179.8	80	Swarm	Aplite	308	10		
181.4	10	Fault	Aplite	283	65		
186.7	40	Fault	Aplite	292	27		
198.2	35	Fracture	Aplite	324	87		19
206.8	10	Fault	Aplite	314	86		
220.8	30	Fault	Äspödiorite	305	58		
223.5	0.5	Fracture	Äspödiorite	305	89		
225.4	0.5	Fracture	Äspödiorite	316	88		
230.4	10	Fault	Äspödiorite	309	88		
234.4	0.8	Fracture	Äspödiorite	289	88		
240.5	0.5	Fracture	Äspödiorite	127	85		10
242.5	10	Fault	Aplite	155	9		18
251.1	5	Fracture	Greenstone	351	26		
258.2	15	Fault	Äspödiorite	288	88		11
259.5	0.5	Fracture	Äspödiorite	322	28		
266.4	10	Fault	Äspödiorite	163	89		
270.3	10	Fracture	Äspödiorite	260	56		
279.1	10	Fracture	Äspödiorite	319	73		
282.2	0.2	Fracture	Äspödiorite	314	59		
285.7	0.5	Fracture	Äspödiorite	290	13		

KA2563A

Location (m)	Width (cm)	Type	Rocktype/ Grout	Strike	Dip	Inflow (l/min)	Associated Structure
12.5	0.2	Fracture	Äspödiorite	335	82		1
16.4	40	Fault	Äspödiorite	284	67		
18.2	5	Fault	Äspödiorite	305	69		
19.8	80	Fault	Aplite	270	75		
56.3	120	Zone	Aplite	11	40		16
68.5	220	Zone	Aplite	135	87		2+3
88.1	5	Fault	Äspödiorite	354	56		
94.4	6	Fracture	Äspödiorite	296	76	40	4
103	2	Fracture	Grout	114	88	700	5
108.9	0.2	Fracture	Aplite	222	34		17
113.6	20	Fault	Äspödiorite	65	32		
116.4	40	Swarm	Aplite	356	63		
117.8	80	Swarm	Aplite	341	88		
121.5	100	Swarm	Aplite	301	56		
129.2	20	Fracture	Aplite	138	78		
131.3	10	Fault	Äspödiorite	68	56		
138.2	10	Fault	Äspödiorite	77	14		
141.3	5	Fault	Grout	97	81		
142.7	5	Fracture	Äspödiorite	313	9		
153.4	140	Fault	Grout	111	73	100	6+7
168.4	30	Fracture	Äspödiorite	280	74		
173.1	5	Fracture	Äspödiorite	286	22		
175.9	7	Fault	Äspödiorite	271	35		
181.2	20	Fracture	Aplite	268	43		
182.6	10	Fracture	Aplite	244	15		
188.7	60	Fault	Äspödiorite	316	82	8	20
190.1	4	Fault	Äspödiorite	323	76		
194.3	0.1	Fracture	Aplite	12	18		18
196.9	2	Fracture	Äspödiorite	53	55		
203.8	40	Fracture	Äspödiorite	7	54		
207	20	Fault	Äspödiorite	321	86		13
213.5	10	Fault	Äspödiorite	323	81		
222.1	0.5	Fracture	Äspödiorite	284	90		
226.8	10	Fault	Äspödiorite	308	47		19
230.7	10	Fracture	Äspödiorite	123	88		
242.4	8	Fault	Äspödiorite	26	67		8
245.5	0.5	Fracture	Äspödiorite	305	54		
253.1	8	Fault	Äspödiorite	8	47		
264.9	10	Fracture	Äspödiorite	346	78		
265.8	5	Fault	Äspödiorite	96	85	1.2	9
291.1	20	Fracture	Aplite	250	27		
306.4	40	Fault	Äspödiorite	246	46		
310.3	20	Fault	Aplite	220	88		
315.2	50	Fault	Äspödiorite	224	82		
321.7	0.2	Fracture	Äspödiorite	229	48		
339.1	10	Fracture	Aplite	121	76		
342.6	80	Fault	Äspödiorite	252	77		
343.7	0.5	Fracture	Äspödiorite	135	89		
344	40	Swarm	Äspödiorite	306	66		
346.4	10	Fracture	Aplite	291	86		
347	80	Swarm	Aplite	202	8		
348	70	Fault	Aplite	242	56		
349	30	Fault	Aplite	247	71		
351.3	25	Fault	Aplite	124	80		
352.7	25	Fracture	Äspödiorite	10	83		
353.5	0.5	Fracture	Aplite	129	87		
354.8	0.5	Fracture	Aplite	224	18		
355.5	0.5	Fracture	Äspödiorite	67	56		

KA3510A

Location (m)	Width (cm)	Type	Rocktype/ Grout	Strike	Dip	Inflow (l/min)	Associated Structure
10.7	0.2	Fracture	Äspödiorite	21	85		
11.1	15	Fracture	Äspödiorite	309	75		2
12.9	8	Fault	Äspödiorite	115	89		4
13.7	15	Fracture	Aplite	154	12		
14.6	5	Fracture	Aplite	270	88		
16.1	100	Zone	Äspödiorite	232	89		8
17.6	10	Fracture	Äspödiorite	323	38		
19.9	20	Fracture	Äspödiorite	59	60		
21.5	5	Fault	Äspödiorite	50	89		
22	35	Fracture	Äspödiorite	291	88		
22.6	40	Fault	Äspödiorite	49	89		
25	10	Fault	Äspödiorite	252	62		
30.9	10	Fracture	Äspödiorite	288	88		
32.6	0.5	Fracture	Aplite	309	17		
36.5	0.5	Fracture	Grout	321	79		
37.5	40	Zone	Grout	106	81		3
43.2	10	Fracture	Äspödiorite	125	70		
47.1	15	Fracture	Äspödiorite	111	82		
47.7	10	Fault	Äspödiorite	138	75	40	5
48.8	25	Fracture	Äspödiorite	230	74		
31.9	2	Fracture	Äspödiorite	165	67		
56.7	0.5	Fracture	Äspödiorite	131	87		6
59	2	Fracture	Äspödiorite	190	73		
61.1	9	Fault	Äspödiorite	164	82		
67	0.2	Fracture	Äspödiorite	230	19		
75.7	22	Fault	Aplite	184	78	0.3	
95.9	10	Fault	Äspödiorite	133	75		
108.2	0.5	Fracture	Äspödiorite	220	17		
112.3	5	Fracture	Aplite	47	76		
112.6	22	Swarm	Aplite	237	46		
113.6	0.5	Fracture	Aplite	183	16		
116.4	10	Fracture	Aplite	271	76		
117	45	Swarm	Aplite	277	87		
118	60	Fault	Aplite	269	88	40	15
119.5	30	Fault	Aplite	98	90		
122.4	5	Fracture	Äspödiorite	147	77		
130.6	0.5	Fracture	Äspödiorite	263	39	0.1	
137.1	0.5	Fracture	Äspödiorite	215	21		
137.8	0.5	Fracture	Äspödiorite	197	10		
140.8	0.5	Fracture	Äspödiorite	254	18		
144.6	0.5	Fracture	Äspödiorite	193	11		
145.8	0.5	Fracture	Äspödiorite	73	49		

KI0025F

Location (m)	Width (cm)	Type	Rocktype/ Grout	Strike	Dip	Inflow (l/min)	Associated Structure
3.8	0.5	Fracture	Grout	301	74		
4.9	10	Fracture	Grout	307	57	40	5
7	15	Fault	Grout	301	68		
29.6	60	Fracture	Greenstone	110	54		
35.6	10	Fault	Äspödiorite	77	87		
37.1	10	Fault	Greenstone	301	82		
43.5	25	Fracture	Äspödiorite	140	78	1.5	7
69.4	10	Fault	Äspödiorite	250	67		
71.9	40	Fault	Aplite	47	81		
76.6	80	Fracture	Äspödiorite	107	65		6
87.1	5	Fracture	Äspödiorite	265	33		
87.7	0.2	Fracture	Aplite	336	77	1.9	20
107.5	50	Swarm	Aplite	212	30		
109	10	Fault	Äspödiorite	240	79		
114.3	40	Fault	Äspödiorite	37	84		
125	250	Fracture	Greenstone	292	72		
146.3	60	Fracture	Äspödiorite	305	20		
150.3	10	Fracture	Äspödiorite	300	41		
154.3	80	Fracture	Äspödiorite	253	84	0.2	
162.3	10	Fracture	Äspödiorite	268	75		
163.9	100	Fracture	Äspödiorite	268	73		
166.4	65	Zone	Äspödiorite	338	74	10	19
167.9	5	Fracture	Äspödiorite	156	90		
171.5	15	Fracture	Äspödiorite	238	90		
180.2	40	Fracture	Aplite	264	69		
188.5	60	Fracture	Aplite	253	85		
187.3	-	Zone	Äspödiorite	219	50	70	
191.1		Zone	Äspödiorite				
192.1	35	Zone	Äspödiorite	243	77		

KI0023B

Location (m)	Width (cm)	Type	Rocktype/ Grout	Strike	Dip	Inflow (l/min)	Associated Structure
2	5	Fracture	Äspödiorite	348	84		
4.7	0.5	Fracture	Äspödiorite	13	89		
6	20	Zone	Äspödiorite	308	71		
7.2	5	Fracture	Äspödiorite	112	87		
31.3	10	Fault	Äspödiorite	338	83	2	
31.7	0.3	Fracture	Äspödiorite	308	86		
39.6	10	Swarm	Äspödiorite	275	22		
42.2	4	Fracture	Äspödiorite	103	87	48	7
42.4	2	Fracture	Äspödiorite	292	28	-"-	
43.7	0.5	Fracture	Äspödiorite	16	80		
44.2	0.5-10	Fracture	Äspödiorite	88	83		6
63.7	5	Fault	Äspödiorite	172	76		
68.9	15	Fault	Äspödiorite	133	89		
69.8	20	Fault	Äspödiorite	157	82	3	20
71.1	10	Fracture	Äspödiorite	123	86		9
75.5	80	Swarm	Äspödiorite	348	41		18
85.6	8-15	Fault	Äspödiorite	318	89		13
87.7	3	Fault	Äspödiorite	179	82		
111.6	20	Fault	Äspödiorite	342	87	3	19
112.1	5	Fault	Äspödiorite	332	85		
112.5	2	Fracture	Äspödiorite	306	88		
116.5	20	Fault	Greenstone	222	64		
140.7	30	Fracture	Aplite	277	23		
151	40	Fracture	Aplite	303	83		
164.6	0.5	Fracture	Äspödiorite	152	89		
166.3	200	Zone	Äspödiorite	298	89		
168.6	10	Fault	Äspödiorite	297	89		
170	10	Swarm	Äspödiorite	300	81		
170.7	30	Zone	Äspödiorite	298	83	18	10
171.1	0.5	Fracture	Äspödiorite	284	77		
174.5	0.2	Fracture	Äspödiorite	298	21		
183.9	10	Fracture	Äspödiorite	275	6		
188.7	5	Fault	Äspödiorite	127	81		
190.4	2	Fracture	Äspödiorite	347	42		
192.7	10	Fault	Äspödiorite	282	72		